

LRP 623/98

November 1998

**High Accuracy Magnetic Field
Measurements with a Hall Probe**

C. Schott, R.S. Popovic,
S. Alberti, M.Q. Tran

submitted for publication in
REVIEW OF SCIENTIFIC INSTRUMENTS

High Accuracy Magnetic Field Measurements with a Hall Probe

C. Schott and R.S. Popovic

Institute for Microsystems (DMT-IMS)

S. Alberti and M.Q. Tran

Centre de Recherches en Physique des Plasmas (CRPP-PPB)

Association EURATOM - Confédération Suisse

Ecole Polytechnique Fédérale de Lausanne, CH-1015 Lausanne, Switzerland

(11/11/98)

Abstract

A silicon based temperature stabilized axial Hall probe with an absolute accuracy of ± 40 ppm in the full range between 0 and 6T is presented. The absolute calibration of the probe is performed against a Nuclear Magnetic Resonance (NMR) probe. The application to the measurement of a magnetic field profile of a 5 T superconducting magnet system, with field gradients as high as 30 T/m, reaching an overall accuracy of better than ± 100 ppm, is demonstrated. In addition to the high absolute accuracy, this Hall probe allows high spatial resolution measurements of inhomogeneous fields in configurations where present NMR probes are not usable.

Typeset using REVTeX

I. INTRODUCTION

For high power mm-wave coherent sources of rf radiation as in gyrotrons or free electron lasers [1], steering and focusing systems in particle accelerators [2], magnetically confined plasmas as in tokamaks or stellarators [3], NMR imaging [4] or spectroscopy systems [5], a magnetic field system is required and is normally generated by either normal conducting coils or by superconducting coils. Depending on the application, the magnetic field can be dc or ac and the field line topology can be fairly complicated as for instance in stellarators or wigglers used in free-electron lasers. Stringent constraints on the accuracy of the absolute value of the magnetic field are also often required for proper operation of the system.

The accurate measurement of magnetic fields can be performed with Nuclear Magnetic Resonance (NMR) probes in the case of field profiles with gradients not exceeding 1-2 T/m, which, for many applications is a severe limitation. When the field line topology is very complicated, indirect techniques are used as for instance electron beams [6] or pulsed wire systems [7] and mainly allow to measure the topology of the magnetic structure or to align the coil system with respect to a fixed reference frame. The most commonly used direct measurement technique is based on Hall probes which can be either single-axis or 3D, the latter being used when the 3 components of the field are simultaneously required. In the range of magnetic fields between 0 and 2 T, the absolute accuracy reached with commercially available magnetometers is of the order of 1 – 2% and can be totally insufficient for many applications where an absolute accuracy of 100-1000 ppm is needed.

In the present paper it is shown that a newly developed axial Hall probe based on silicon technology and calibrated against a NMR probe can reach an absolute accuracy of the order of ± 40 ppm in the range from 0 to 6T. A second important feature of the Hall probe, compared to a NMR probe, is the possibility of measuring highly inhomogeneous fields with a good spatial resolution.

This paper is organized as follows: after the introduction, the Hall probe configuration and the intrinsic physical limitations of the accuracy of magnetic field measurements are

presented. The experimental setup as well as the absolute calibration procedure and an error estimation are given in the following section. An example of magnetic field measurement in a 5 T superconducting magnet used for high power mm-wave generation (118 GHz) with a gyrotron [8] is then presented. Finally, the experimental results will be discussed and summarized.

II. HALL PROBE CONFIGURATION

The magnetic field measurement is carried out using a modified commercial SENTRON Hall transducer (Sentron Model ZS150 3-5-2T), which was developed in collaboration with the Institute of Microsystems of the Ecole Polytechnique Fédérale de Lausanne. The entire measurement setup is shown in figure 1. The transducer contains two parts, the magnetic field sensitive probe-head and the electronic interface. It is powered by a standard $\pm 12V$ laboratory power supply and its output voltage is read by a Keithley Model 182 sensitive digital voltmeter. For temperature stabilization a Lakeshore Model 340 Temperature Controller was used. For absolute calibration of the magnetometer a Metrolab Model PT 2025 precision NMR-meter with five NMR probes and a multiplexer switch was used. NMR meter and Digital Voltmeter were connected via the GPIB interface bus to a personal computer to allow for automatic data acquisition and signal correction via the LabView software package. As shown in figure 2a, the active volume of the probe head is located at one tip and is of very small dimensions ($1 \times 0.3 \times 0.2 \text{ mm}^3$). Figure 2b gives a schematic view of the probe head incorporating two Hall devices, heating foils and temperature sensors.

Contrary to most Hall probes for high precision magnetometry which have to date been based on Hall generators made of high-mobility compound semiconductors, such as InSb and GaAs, the sensors in the SENTRON transducer are made of silicon. Theoretically, a high carrier mobility is crucial for achieving high sensitivity, low offset, and low noise. However, the application of compound materials implies several drawbacks, including the use of a very specific niche technology, considerable long-term instability, high temperature

cross-sensitivity and high non-linearity at higher magnetic fields. Silicon is not a high carrier mobility material, but it offers many other advantages compensating for this drawback. The silicon Vertical Hall Sensor [9], used in the Sentron probe, features extremely high long-term stability with sensitivity changes less than 10^{-4} over 10 years. The geometry of the vertical Hall sensor is obtained from a classical rectangular Hall plate by a conformal transformation which makes all contacts to appear on one side [10]. This feature is ideal for microelectronic fabrication methods, so that the sensors can be made very small and a good spatial resolution is achieved. Large series fabrication of the device and the application of highly sophisticated and mature silicon technology result in narrow tolerances for parameters like Hall coefficient, offset, geometry related coefficients and noise.

The Sentron Hall probe contains two Hall devices in the probehead for the reason of offset reduction by mutual cancellation. The two sensors are selected elements featuring similar offset, assembled in such a way, that they see an applied field from opposite direction. Thus for one sensor offset adds to the Hall voltage and for the other it is subtracted from it, resulting in a very low residual offset when the two output signals are combined [11]. Reducing offset is essential for high accuracy measurements, since offset is directly related to the material resistivity, a parameter which changes with temperature and magnetic field.

For the accurate measurement of fields higher than a few mT, non-linearity becomes a concern. For the vertical Hall device it composes of three distinct effects [12]. The first is called junction-field effect and describes the modulation of the width of the active zone of an integrated Hall device. The second is related to the device geometry, in particular the length to width ratio of the device and the contact lengths. The third effect is due to the scattering mechanisms of the material resulting from the interaction between charge carriers and crystal lattice. All three effects together sum up in an overall non-linearity of the probe, which in our case is corrected by calibration towards a high precision NMR meter. Since silicon Hall devices have a temperature dependence of the sensitivity of approximately $0.08\%/^{\circ}\text{C}$, for highly accurate measurements temperature has to be stabilized. For this reason the probe head was equipped with a heating foil and a temperature sensor for each of the two ceramic

supports carrying a Hall sensor (Figure 2b). The ceramic plates can only be heated, so the temperature is stabilized at 40°C, which is under any circumstances above environmental temperature. The temperature stabilization was implemented using a closed-loop Lakeshore 340 temperature controller. Testing showed that the maximum temperature fluctuation could be kept inferior to 0.01°C, which is equivalent to a temperature cross-influence of smaller than 10ppm. The probe showed a magnetic field sensitivity of about 1.1 V/T and a non-linearity of about -2% at a field of 6T as shown in figure 3.

Another important point for the use of magnetometers is the frequency response. The good stability of the sensors and the pure analog electronic signal treatment inside the transducer assure an output signal in phase with the applied field for a wide range of frequencies. Figure 4 shows such a measurement, performed at a field of 10mT and one observes a sensitivity flatness up to frequencies of several kHz. Theoretically the Hall effect in silicon develops until frequencies of the order of magnitude of THz, but practically the bandwidth is limited to much lower values by parasitic capacitances inside the device itself as well as inside the electronic components used for analog signal treatment.

III. EXPERIMENTAL SETUP AND CALIBRATION PROCEDURE

In this section the experimental setup will be outlined. In part A the superconducting coil configuration as well as the magnetic field properties for the probe calibration will be described, in part B the calibration procedure will be outlined and in part C the errors of the system will be estimated.

A. Magnetic Field Configuration

For performing the Hall probe calibration against a NMR probe in the full range between 0 and 6 T, the properties of the magnetic field configuration had to fulfill simultaneously two criteria: first, the NMR-meter requires a field homogeneity better than 1T/m and second, the field had to be swept in the full range between 0 and 6T. The type of magnet satisfying

simultaneously these two constraints are typically used in gyrotrons for mm-wave generation. The superconducting coil configuration (ACCEL Instruments) is shown in figure 5 and is composed of four solenoids wound on a common mandrel. In this figure the coils B3 and B4 are the main coils, generating a highly homogeneous field (10^{-3}T/mm^3) in a volume defined by a cylinder of 50mm height and 20mm radius, with its center located on the axis of the coil system with an axial position indicated on the figure by $z_c = 435$ mm. For controlling the electron beam optics used in the gyrotron, the two coils B1 and B2 allow the control of the magnetic field profile outside the homogeneous region. The warm bore centered on the magnetic axis is of 140mm in diameter and is open at both top and bottom of the cryostat. For optimum tuning of the gyrotron operation, the required accuracy on the magnetic field control has to be of the order of 1000ppm, and the magnetic axis alignment with respect to the mechanical axis defined by the warm bore has to be better than 0.1mm along the entire warm bore. For energizing the different coils, highly stable power supplies (OXFORD IPS120-10) have been used. At a maximum current of 120A corresponding to a magnetic field around 6.5T, the current setting resolution is 1mA with a current stability of $\pm 3\text{mA}$. The calculated on axis z-component of the magnetic field, $B_z(z)$, as well as the field gradient $\partial B_z/\partial z$ are shown in Figure 6. The probe holder used for the calibration allowed to place simultaneously the active parts of the Hall and NMR probes at the same axial position ($\pm 0.5\text{mm}$) but both placed radially of axis ($r = 3 \pm 0.2$ mm) with an azimuthal separation of 180° . The error in magnetic field associated to the ± 0.2 mm radial positioning accuracy is about $\pm 5\text{ppm}$, which is well below the achieved accuracy. The accuracy of the NMR probe is also of the order of ± 5 ppm.

B. Calibration procedure

In order to obtain the value of the measured magnetic field, the voltage, V_{Hall} , from the Hall transducer has to be corrected. The uncorrected sensitivity curve in figure 3 suggests to use a polynomial function for $B(V_{Hall})$. The polynomial coefficients were set after a

calibration run, where the Hall probe signal was referenced to a NMR signal over the field range of interest between 0.2 and 6 Tesla. Although Hall sensors show theoretically a symmetrical behavior for positive and negative field orientations, small irregularities during fabrication and assembly give rise to variations of offset and sensitivity of the device making it slightly asymmetrical. This requires a calibration for both field directions. We used the LabView standard procedure "General Polynomial Fit.vi" to perform the fit on the 9th order polynomial. The solving algorithm applied is the "Singular Value Decomposition" [13] which is very efficient and stable in the case of over-determined systems. It is frequently used when the number of data points is higher than the order of the polynomial, so that the best fit can be chosen in the least-square sense.

C. Error estimation

After the description of the measurement system and the field generating system, the different error sources have to be evaluated to determine the measurement accuracy. We can basically distinguish between geometrical errors, modelling errors and stability errors.

A first geometrical error is caused by the tolerances of the absolute position of the Hall devices inside the probe head and by positioning the probe head inside the coil system. These two tolerances sum up to a total positioning error of about 0.2 mm for our system, resulting in a virtual shift of the magnetic flux density along the z-axis. A second geometrical error is induced by the fact that the active volume is not infinitely small. This error is only important in parts along the z-axis, where the field gradient is non-constant, since the error is proportional to the second derivative of the field. A first modelling error is introduced by the limited accuracy of the polynomial fit to the measured Hall data, and a second by the fact, that offset and temperature were drifting during the calibration procedure. The total of these two errors can be checked by comparing NMR data to corrected Hall data in a separate measurement after calibration as shown in figure 7 for positive and negative field orientations.

Stability errors are caused by time dependent offset drift and temperature dependent sensitivity drift of the sensors, as well as by the limited accuracy of the NMR-meter, which serves as absolute reference. The influence of an unstable supply current in the coils of $\pm 3\text{mA}$, which corresponds to about $\pm 25\text{ppm}$ around the field center, does not create an error, because this variation is part of the actual measurement value.

All these error sources have been estimated and table I shows how much each of them contributes to the total error, which adds to about $\pm 90\text{ppm}$. Since there is no predominant error source, the system can be described as well balanced. However, for improving accuracy for example one order of magnitude, all errors have to be reduced.

IV. EXPERIMENTAL RESULTS

The complete measurement of the on axis component between $z = 0\text{m}$ and $z = 0.66\text{m}$ has been performed with the calibrated probe. As shown in figure 6 the magnetic field varies between 0.2 and 4.5T and the maximum on axis field gradient is of the order of 30 T/m. This gradient is almost two orders of magnitude higher than the maximum gradient allowed for NMR probe measurements. The comparison between calculated on axis profile and measured values is shown in Figure 8. In this figure, the calculated values are indicated by the dotted line, and the relative difference between theory and measurement is indicated by the squares. In the flat region section ($z = 435 \pm 25 \text{ mm}$), which is of particular importance for the gyrotron operation, this error is significantly lower than the specified value of 500 ppm. Outside the flat field region, the accuracy of the measurement is slightly degraded in the regions where the second derivative of the field is maximum ($z \simeq 200\text{mm}$ and $z \simeq 580\text{mm}$) due to the finite probe size. The maximum measurement error in these regions has been evaluated to $\pm 250\text{ppm}$ which is significantly lower than the measured deviation. These deviations could be caused by minor deformations of the superconducting coil windings under the radial magnetic forces [14].

An off axis measurement of the B_z component, required for defining the magnetic field

homogeneity in the flat region, is shown in figure 9. In this figure, the continuous line shows the calculated off axis ($r = 25\text{mm}$) B_z component for the ideal system where the magnetic axis corresponds to the mechanical axis. The squares are an average value of the measured quantity where the average has been taken on 6 different azimuthal positions (every 60°) for every z position. A qualitative measure of misalignment of the mechanical axes with respect to the magnetic axis is given by the rms value of the B_z component where the rms quantity is again calculated on the 6 azimuthal positions for every z position. By making an azimuthal scan of the probe placed off axis ($r = 25\text{ mm}$) at the axial positions where the field gradient $\partial_r B_z$ is maximum ($z = 190\text{ mm}$ and $z = 640\text{ mm}$), it has been determined that the magnetic axis is inside a cylinder of radius of 0.15 mm (centered on the mechanical axis) and length of 660 mm (between $z = 0\text{ mm}$ and $z = 660\text{ mm}$).

V. CONCLUSIONS

High accuracy magnetic field measurements with a silicon based single-axis Hall probe in the full range between 0 and 6T have been demonstrated. An accuracy of $\pm 40\text{ppm}$ for the probe and an estimated accuracy of better than $\pm 100\text{ppm}$ for the entire setup was reached. Magnetic field profiles with gradients up to 30T/m have been measured. Compared to NMR probes, which typically reach an accuracy one order of magnitude better, the Hall probe allows for measurements in highly non-homogeneous fields. In addition to that it is possible to use one single calibrated Hall probe to measure magnetic fields from practically zero to the highest magnetic field values presently generated, where with NMR probes, for covering the same range, an important number of different probes (5 in our case) is needed. Magnetic field transducers with identical Hall sensors have been used in fields up to over 30 Tesla for the scan of very high field resistive magnets in the National High Magnetic Field Laboratory, Tallahassee, USA [15]. The nonlinearity of the output voltage with the magnetic field under these conditions can equally be approximated by a polynomial, so that the same approach as here can be made to obtain accurate data with a Hall magnetometer.

Development of 3D Hall probes with similar accuracy is presently under progress.

ACKNOWLEDGMENTS

T. Centra provided invaluable technical assistance. This work was partially supported by the Fonds National Suisse pour la Recherche Scientifique, as well as by the Swiss priority program MINAST. Support from R. Kreutz, M. Schillo and J. Hobl of ACCEL Instruments GmbH (Bergisch-Gladbach, Germany) and from R. Racz of SENTRON (Zug, Switzerland) is gratefully acknowledged.

REFERENCES

- [1] J. Benford and J. Swegle, *High-Power Microwaves*, (Artech House 1991), Chapters 7 and 8.
- [2] D.A. Edward and M.J. Syphers, *An introduction to the physics of High energy particle accelerators*, (Wiley Interscience 1993).
- [3] K. Miyamoto, *Plasma Physics For Nuclear Fusion*, (The MIT Press 1989), Chapter 2.
- [4] M.A. Brown and R.C. Semelka, *MRI: Basic Principles and Applications*, (Wiley-Liss 1995).
- [5] H. Friebolin, *Basic One and Two-Dimensional NMR Spectroscopy*, (Wiley-Liss 1995).
- [6] E. Ascasibar, J. Qin, A.L. Fraguas, I. Pastor, J. Herranz, Nucl. Fusion 37, 851 (1997).
- [7] R.W. Warren, Nucl. Instrum. Methods Phys. Res. A 272, 257 (1960).
- [8] C. Tran, E. Giguët, P. Thouvenin, P. Garin, M. Pain, S. Alberti, M.Q. Tran and M. Thumm, in *Proceedings of 23rd International Conference on Infrared and Millimeter Waves*, Colchester, UK, 1998, edited by T.J. Parker and S.R.P. Smith, ISBN 0 9533839 0 3.
- [9] R.S. Popovic, IEEE-EDL 5, 357 (1984).
- [10] R.S. Popovic, *Hall Effect Devices*, Adam Hilger (now IOP, the Institute of Physics Publishing), Bristol, Philadelphia and New York, 1991.
- [11] Ch. Schott, H. Blanchard, R. S. Popovic, R. Racz and J. Hrejsa, IEEE Trans. Instrumentation and Measurement 46, 613 (1997).
- [12] Ch. Schott and R. S. Popovic, Transducers 97, Chicago, USA, June 16-19, 1997.
- [13] W.H. Press, S.A. Teukosky, W.T. Vetterling, B.P. Flannery, *Numerical Recipes in C, Second Edition*, (Cambridge University Press 1992), Chapter 2.6.

- [14] R. Kreutz, (private communication 1998).
- [15] M.D. Bird, S. Bole, Y.M. Eyssa, B.J. Gao and H.-J. Schneider-Muntau, IEEE Transactions on Magnetics **4**, 2444 (1996)

TABLES

TABLE I. Error sources in the region between $z = 420 - 450\text{mm}$

Error source	error	abs. error	rel. error [ppm]
absolute position error	$\pm 0.2\text{ mm}$	$\pm 80\text{ }\mu\text{T}$	< 20
size of sensitive volume	0.2 mm	$\pm 50\text{ }\mu\text{T}$	< 15
sensor offset drift 12h	$\pm 30\text{ }\mu\text{T}$	$\pm 30\text{ }\mu\text{T}$	< 10
temperature variations	$\pm 30\text{ mK}$	$\pm 45\text{ }\mu\text{T}$	< 10
calibration of Hall probe	$< 30\text{ ppm}$		< 30
accuracy of NMR	$< 5\text{ ppm}$		< 5
total error			< 90

FIGURES

FIG. 1. Magnetic measurement set-up including Hall transducer, power supply, voltmeter, temperature controller and PC.

FIG. 2. Figure a). Overall layout of the probe head with details of the position and volume of the active part. Figure b) Details of the probe head: two Hall sensors are mounted on ceramic substrates as support plates, the heating foils are fixed on the outside and the standard 100W RTD platinum temperature sensors are fixed on top of these.

FIG. 3. Measured Hall probe sensitivity versus magnetic field.

FIG. 4. Frequency response of the Hall probe system measured at a magnetic field of 10mT.

FIG. 5. Superconducting coil configuration used for calibration of the Hall probe as well as for different field properties. All dimensions are in mm. The coil current densities of the 4 coils B_1 to B_4 are $I_1 = 115.248 \text{ A/mm}^2$, $I_2 = -153.803 \text{ A/mm}^2$, $I_3 = 120.588 \text{ A/mm}^2$, $I_4 = 118.530 \text{ A/mm}^2$, respectively.

FIG. 6. Calculated on axis magnetic field $B_z(z)$ and gradient $\partial B_z / \partial z$ for the coil configuration shown in figure 5.

FIG. 7. Relative deviation between the magnetic field value measured with the NMR meter and Hall data corrected by the polynomial fit. This measurement has been performed with both probes placed in the homogeneous part of the magnetic field.

FIG. 8. Dotted line is the calculated on axis field $B_z(z)$ and the squares are the relative difference between theory and experiment.

FIG. 9. $B_z(z)$ component measured of axis at a radius of $r = 25\text{mm}$ (squares). The continuous line is the theoretical value. The diamonds indicate the rms value taken on 6 different azimuthal positions (every 60°) at each z-position.

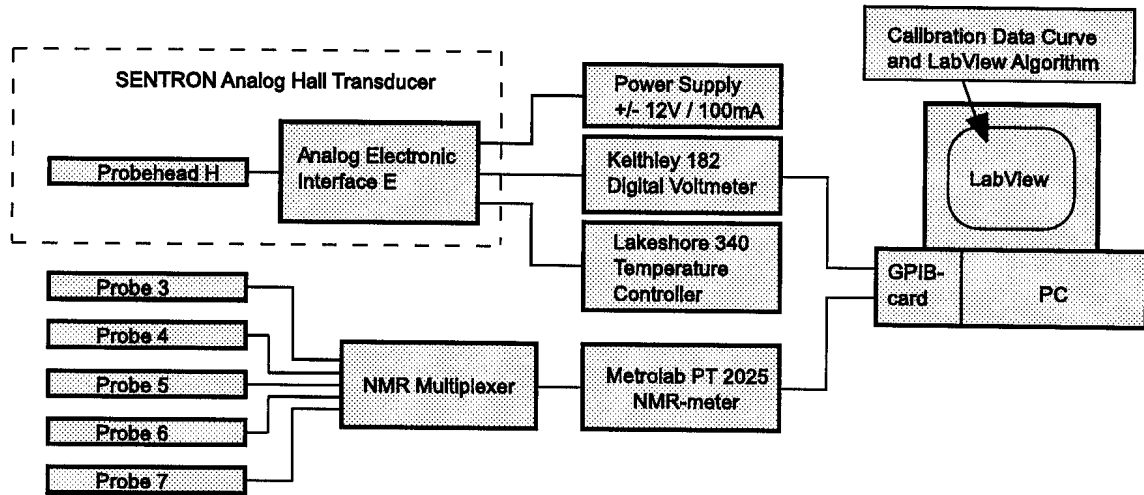


FIG. 1. Magnetic measurement set-up including Hall transducer, power supply, voltmeter, temperature controller and PC.

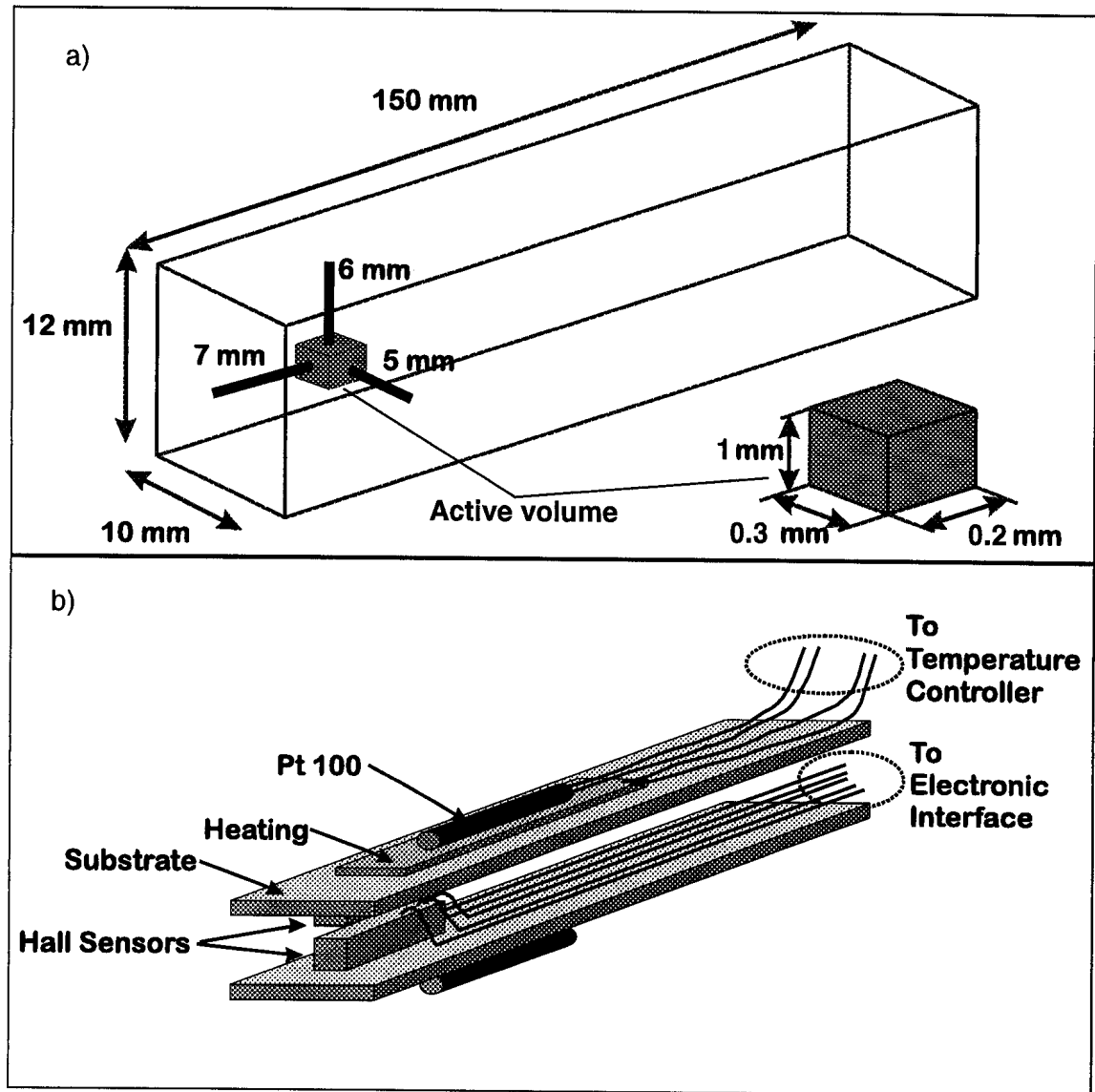


FIG. 2. Figure a). Overall layout of the probe head with details of the position and volume of the active part. Figure b) Details of the probe head: two Hall sensors are mounted on ceramic substrates as support plates, the heating foils are fixed on the outside and the standard 100W RTD platinum temperature sensors are fixed on top of these.

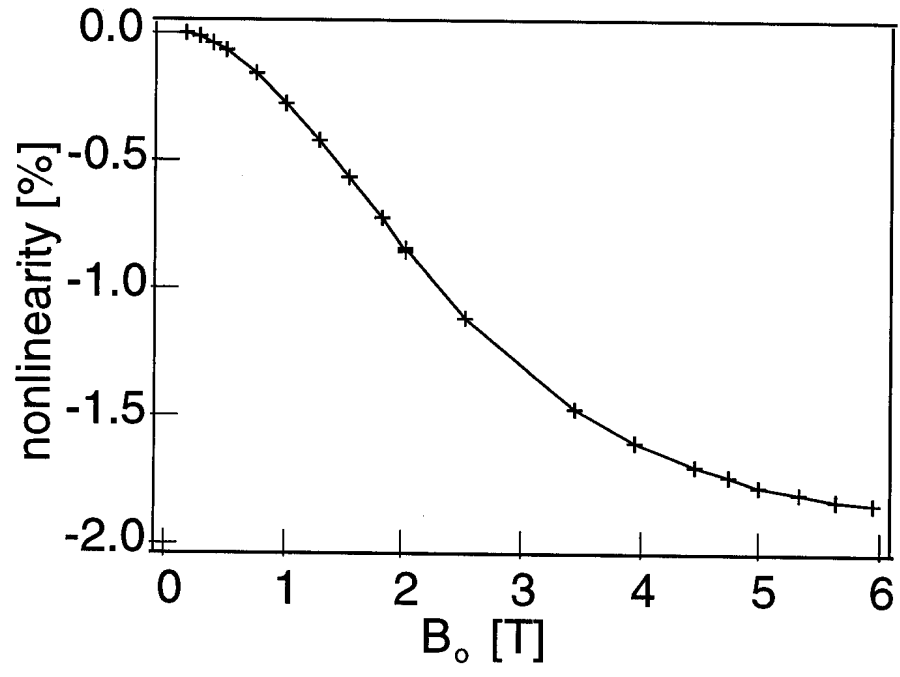


FIG. 3. Measured Hall probe sensitivity versus magnetic field.

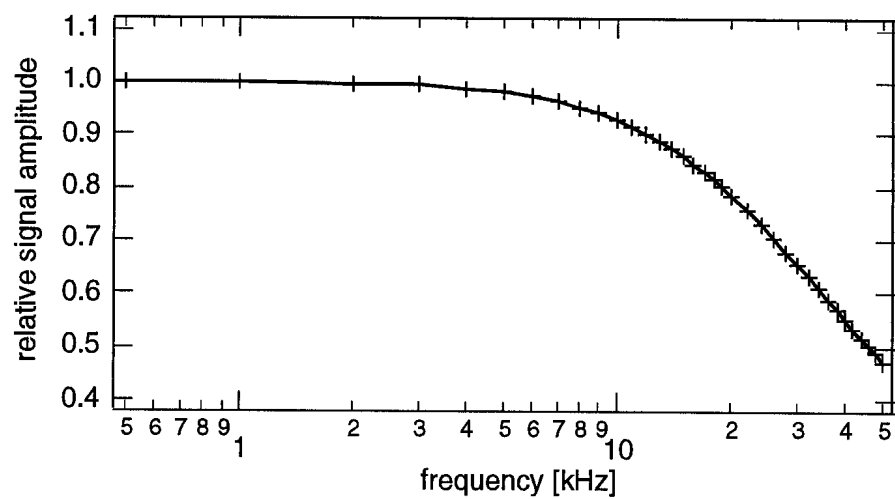


FIG. 4. Frequency response of the Hall probe system measured at a magnetic field of 10mT.

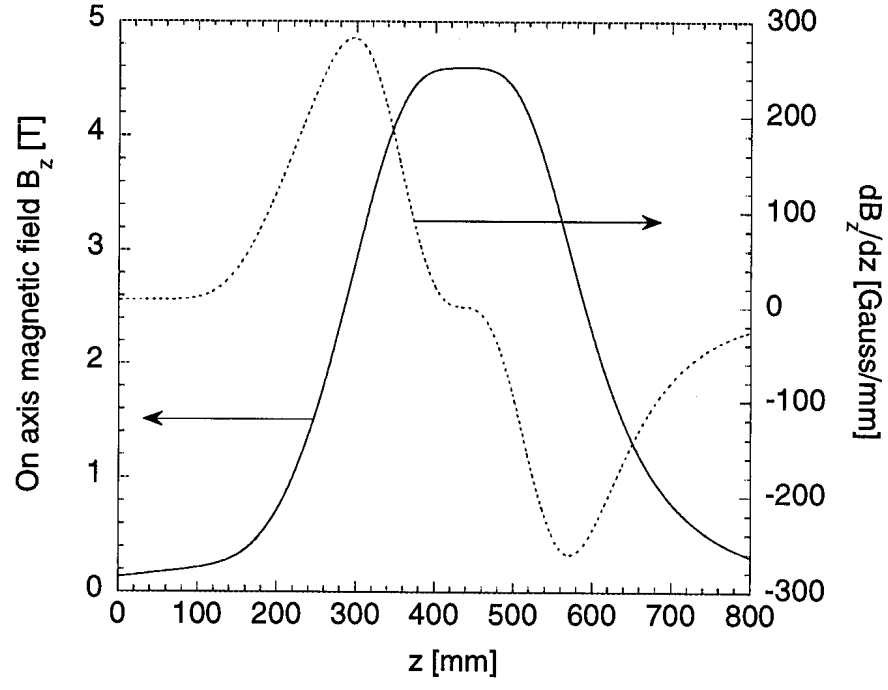


FIG. 6. Calculated on axis magnetic field $B_z(z)$ and gradient $\partial B_z/\partial z$ for the coil configuration shown in figure 5.

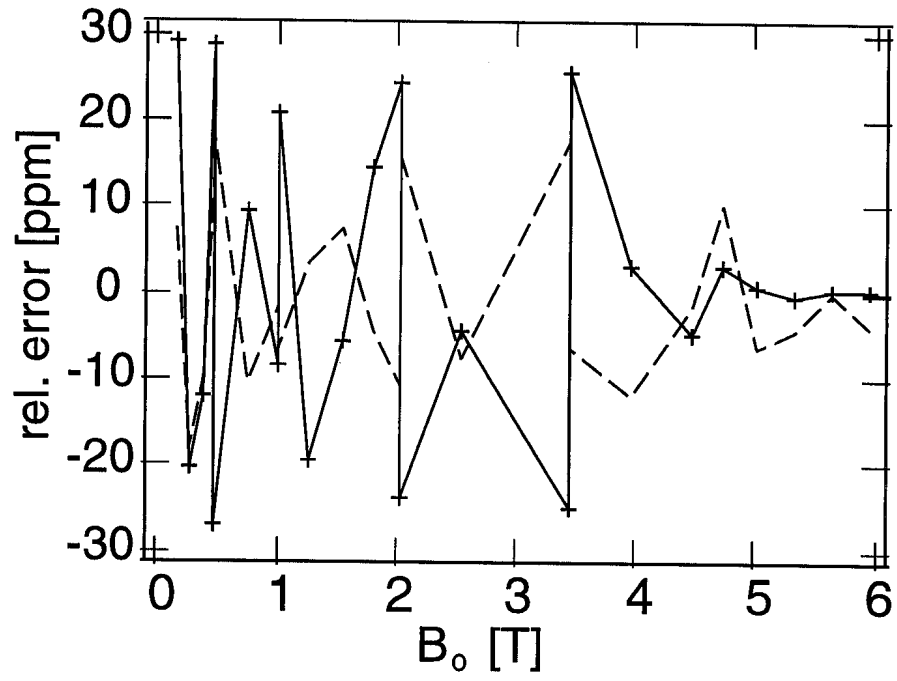


FIG. 7. Relative deviation between the magnetic field value measured with the NMR meter and Hall data corrected by the polynomial fit. This measurement has been performed with both probes placed in the homogeneous part of the magnetic field.

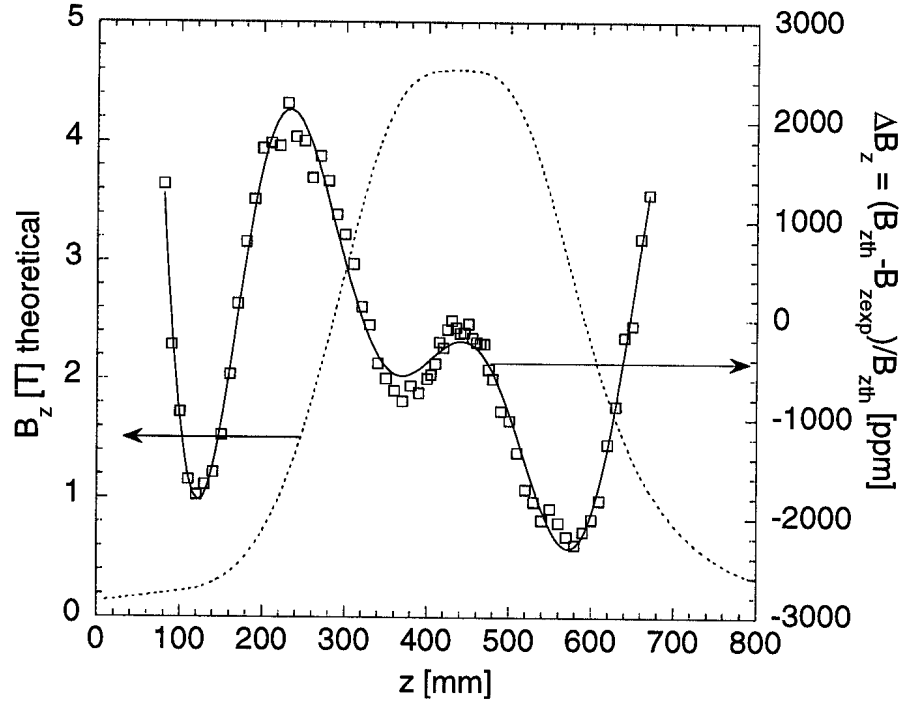


FIG. 8. Dotted line is the calculated on axis field $B_z(z)$ and the squares are the relative difference between theory and experiment.

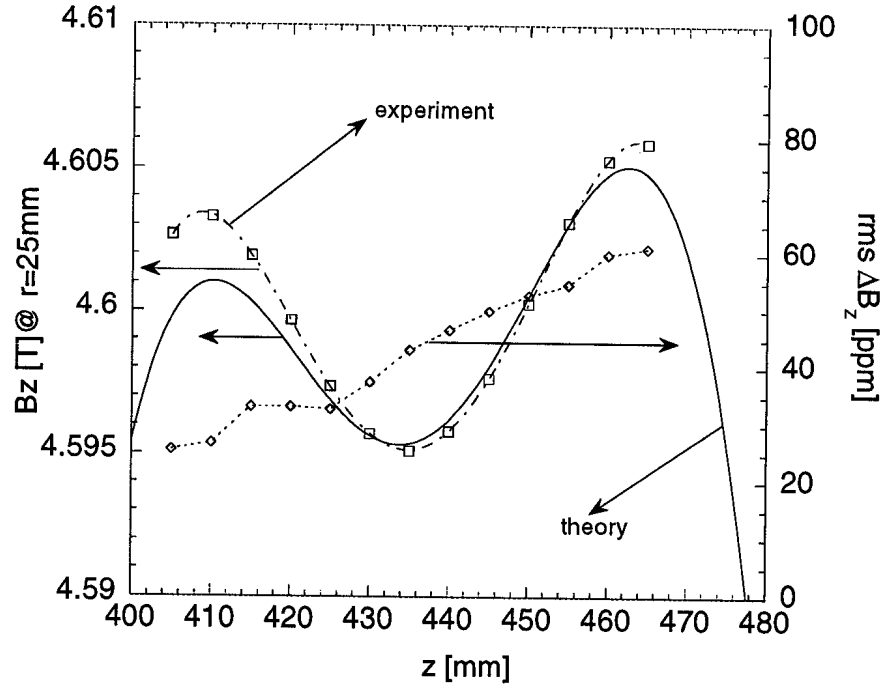


FIG. 9. $B_z(z)$ component measured of axis at a radius of $r = 25\text{mm}$ (squares). The continuous line is the theoretical value. The diamonds indicate the rms value taken on 6 different azimuthal positions (every 60°) at each z -position.

